Anal. Bioanal. Electrochem., Vol. 9, No. 8, 2017, 956-968

Analytical & Bioanalytical Electrochemistry

2017 by CEE
www.abechem.com

Full Paper

Determination of Norepinephrine at a Graphite Screen Printed Electrode Modified with Ag(I) Nanocomplex

Elaheh Movahedi* and Alireza Rezvani[*]

Department of Chemistry, University of Sistan and Baluchestan, Zahedan, P.O. Box 98135-674, Zahedan, Iran

*Corresponding Author, Tel.: +98 54 33447010; Fax: +98 54 33443388

E-Mail: mohahedielaheh@gmail.com

Received: 19 September 2017 / Received in revised form: 8 October 2017 / Accepted: 10 October 2017 / Published online: 31 December 2017

Abstract- A novel nanosensor has been constructed based on nanocomplex with silver, $([Ag(dian)_2]NO_3$, where dian is N-(4,5-diazafluoren-9-ylidene)aniline, modified graphite screen printed electrode (Ag(I)/SPE). The Ag(I) nanocomplex have been prepared by ultrasonic method and characterized structurally by elemental analysis, IR spectroscopy and ^{1}HNMR. Moreover, as a nanosensor for the determination of norepinephrine the Ag(I)/SPE exhibited excellent electrocatalytic activity for the oxidation of norepinephrine with a faster electron-transfer rate. The prepared Ag(I)/SPE were investigated using cyclic voltammetry (CV) and differential pulse voltammetry (DPV). The DPV technique was used for the trace determination of norepinephrine. The oxidation peak currents increased linearly with concentration over the range of 1.0-300 µM, with the detection limit of 0.6 µM for norepinephrine.

Keywords- Norepinephrine, Ag(I) nanocomplex, Graphite screen printed electrode, Voltammetry

1. INTRODUCTION

Neurotransmitters control the physiological and behavioural conditions in human beings by regulating communication within the neural network. These molecules are involved in a large variety of neurophysiological processes including learning, sleep, memory and appetite.

Damage in secretion or uptake of neurotransmitters is known to cause neurodegenerative diseases, drug addiction, and depressive syndromes [1]. Among various neurotransmitters, one important catecholamine norepinephrine (NEP) play essential role in the mammalian central nervous system (CNS). Norepinephrine is a significant transmitter which regulates blood pressure, emotional arousal, and mood disorders. It promotes the conversion of glycogen to glucose in the liver and helps in converting the fats into fatty acids, resulting in an increment in energy production. The norepinephrine is responsible for the increased heart rate, dilation of pupils, dilation of air passages in lungs and narrowing of blood vessels due to which body is able to perform well in stressful situations [2-4]. Knowledge of the concentrations of plasma catecholamine and their metabolites is often useful for diagnosis and evaluation of therapeutic and pharmacodynamic effects for neurological, psychiatric and cardiovascular disorders. Considerable efforts have been made to develop reliable methods for the detection of norepinephrine which is structurally similar and often coexist in biological samples [5-8]. Therefore, the development of an efficient electrochemical sensor to monitor and determine catecholamine in real samples is very important for non-invasive disease diagnosis and pharmaceutical applications. Electrochemical method has been widely used due to its higher sensitivity, selectivity, reproducibility, less time consumption and low cost [9-13].

Screen-printed electrodes (SPE) have attracted considerable attention in recent years because they generally offer beneficial attributes over the traditional electrodes, such as they are portable, field-based size and cost-effective sensors which offer true potential for application in-the-field [14,15]. SPE are inexpensive to manufacture which allows them to be disposable. This aspect is clearly important when testing biological samples and thus avoids surface fouling complications [16]. Unfortunately, the bare electrode usually suffer from a slow response and low reproducibility. This is probably due to relatively low electron-transfer rates are obtained at the surface of such electrodes because of the low diffusion coefficient of the analytes in the electrode [17]. Hence, it is significantly important to develop new materials with excellent properties and suitable designs to gain modified electrode owning superior performance [18]. Most of the modified electrodes are platinum, silver and gold [19].

In the past decades, the investigations on the direct electrochemistry and electrochemical applications of metal nanoparticles have aroused considerable interest in analytical chemistry and bioinorganic chemistry. Silver is one of the most widely used nanoparticles especially in medical science. A great deal of research has been done on different applications of silver nanoparticles in various fields of science, especially in the health area. Some of the most important applications of silver nanoparticles are their usage in cancer treatment, drug delivery and the sensor science [20-23].

According to the previous points, it is important to create suitable conditions for analysis of norepinephrine in biological fluids. In this study, we describe application of novel Ag(I) nanocomplex as a nanostructure sensor for voltammetric determination of epinephrine. The proposed sensor showed good electrocatalytic effect on epinephrine. The modified electrode shows advantages in terms of selectivity, reproducibility and sensitivity. Eventually, we evaluate the analytical performance of the suggestion sensor for norepinephrine determination in drug sample.

2. EXPERIMENTAL

2.1. Apparatus and chemicals

The electrochemical measurements were performed with an Autolab potentiostat/galvanostat (PGSTAT 302N, Eco Chemie, the Netherlands). The experimental conditions were controlled with General Purpose Electrochemical System (GPES) software. The screen-printed electrode (DropSens, DRP-110, Spain) consists of three main parts which are a graphite counter electrode, a silver pseudo-reference electrode and a graphite working electrode.

All solutions were freshly prepared with double distilled water. Norepinephrine and all other reagents were of analytical grade and were obtained from Merck chemical company (Darmstadt, Germany). The buffer solutions were prepared from orthophosphoric acid and its salts in the pH range of 2.0-9.0.

Carbon, hydrogen and nitrogen contents (CHN Microanalysis) were determined on Eager 300 Summarize elemental analyzer. Molar conductance (in Ω^{-1} cm^2mol^{-1}) was measured at room temperature on Systronics Conductivity Bridge 305, using a conductivity cell of 1.0 cell constant. IR spectrum was recorded on a FT-IR JASCO 680-PLUS spectrometer (20 spectra/sec, 16 cm^{-1} resolution, MCT-W detector) using KBr pellets from 4000-400 cm^{-1}. The ^{1}HNMR spectra were acquired using a Bruker 300 spectrometer which set at room temperature.

2.2. Synthesis

2.2.1. Synthesis of ligand, N-(4,5-diazafluoren-9-ylidene)aniline (dian)

The ligand was prepared with method reported before [24] starting with 4,5-diazafluoren-9-one (dafone). The yield was 40%. Elemental analysis: Calc. for $C_{17}H_{11}N_3$: C, 79.36; H, 4.31; N, 16.33. Found: C, 79.50; H, 4. 17; N, 16.59.

2.2.2. Synthesis of nanocomplex, [Ag(dian)$_2$]NO$_3$

A high-density ultrasonic probe was immersed directly into an ethanolic solution of dian (0.51 gr, 2 mmol), elaborating at 20 kHz with a power output of 100 W for 30 min. The temperature was remained constant at 50 °C using an ice bath. Into this solution, 3 ml of $AgNO_3$ solution (0.17 g, 1 mmol) in ethanol was gradually added and sonochemically irradiated with same power for 30 min. Finally, diethyl ether was added dropwise under ultrasonic irradiation to the resultant yellow solution and the suspension irradiated for another 30 min. The acquired precipitate was filtered off, rinsed with cold ethanol and diethyl ether and then air dried (Fig. 1). The yield was 67%. Elemental analysis: Calc. for $C_{34}H_{22}AgN_7O_3$: C, 59.66; H, 3.24; N, 14.32; O, 7.01; found: C, 59.96; H, 3.44; N, 14.02; O, 7.12.

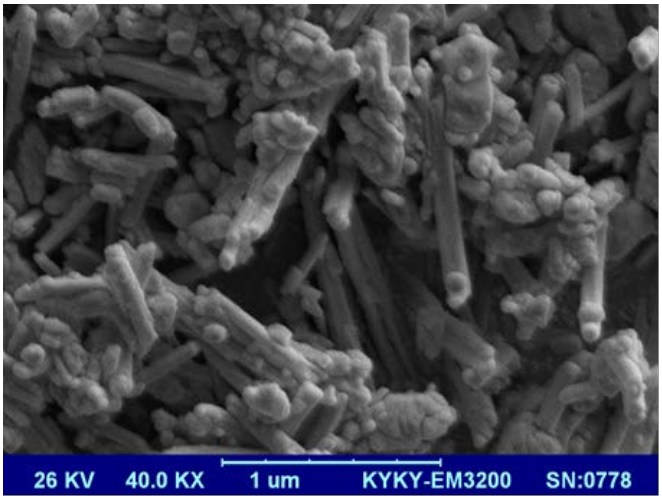

Fig. 1. SEM image of Ag(I) nanocomplex

2.3. Preparation of modified electrode

The bare graphite screen printed electrode was coated with Ag(I) nanocomplex as follows. A stock solution of Ag(I) nanocomplex in 1 ml aqueous solution was prepared by dispersing 1 mg Ag(I) nanocomplex with ultrasonication for 1 h, and a 5 µl aliquot of the Ag(I) nanocomplex/H_2O suspension solution was casted on the carbon working electrodes, and waiting until the solvent was evaporated in room temperature.

3. RESULTS AND DISCUSSION

3.1. Synthesis and structural analysis

The synthetic procedures for the ligand and nanocomplex are depicted in scheme 1. The dian ligand has been prepared previously and fully characterized with crystallographic and spectroscopic data [24,25]. The X-ray crystal structure of it reveals that the 4,5-diazafluorenylidene unit is nearly planar which oriented at a dihedral angle of 75.75 (3)˚ with respect to the phenyl ring.

The d^{10} Ag(I) ion has no electronically imposed preference for any particular coordination geometry. Structures of Several Ag(I) complexes with 1,10-phenanthroline [26] ligand and its derivatives such as 4,5-diazaflourene [27] and 1,10-phenanthroline-5,6-dione [28] were reported and from these results, with two hetero-aromatic chelating ligand can expect diverse geometries for Ag(I) nanocomplex such as pseudo square-planar, distorted tetragonal pyramid, and pseudo-tetrahedral structure. For our newly synthesized nanocomplex several attempts failed to obtain a single crystal suitable for X-ray crystallography. Though, the spectroscopic and analytical data enable us to predict the possible structure (Scheme 1).

Spectral data (IR, ^{1}HNMR) and CHN analysis were consistent with the proposed formulation of the nanocomplex. The synthesized Ag(I) nanocomplex has good solubilities in most of the ordinary solvents. The obtained molar conductance value of 59.3 $ohm^{-1}cm^2mol^{-1}$ in DMSO (10^{-3}M) at room temperature indicates that Ag(I) nanocomplex is 1:1 electrolyte. It must be noted that conductance values in the range of 50 to 70 $ohm^{-1}cm^2mol^{-1}$ are suggested for 1:1 electrolytes in DMSO [29]. The nitrate ion was found not to be coordinated to the metal ion as confirmed by conductivity measurements and FT-IR data.

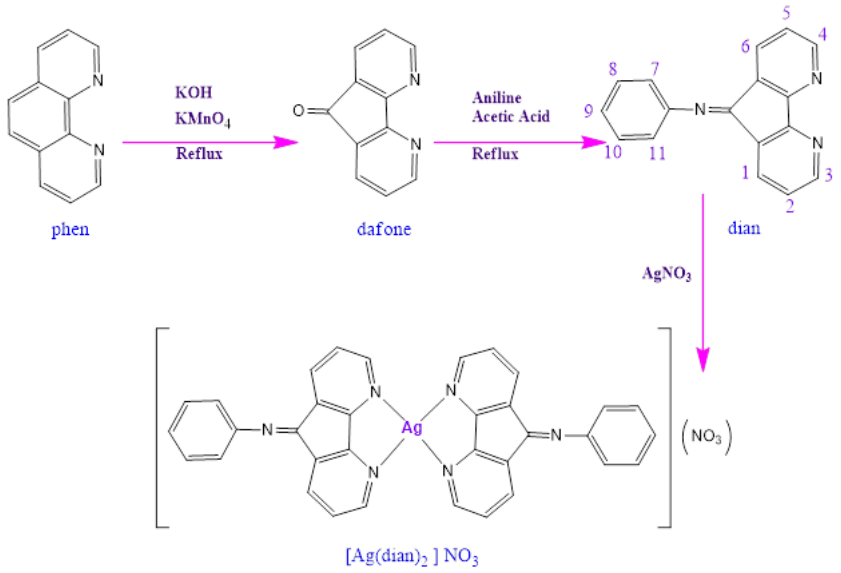

Scheme 1. Synthesis of $[Ag(dian)_2]NO_3$

3.2. Spectroscopic Parameters

3.2.1. IR Spectral Studies

The FT-IR spectrum of free ligand (N-(4,5-diazafluoren-9-ylidene)aniline) (Fig. 2) exhibits the characteristic bands of the 3048 (CH, ar.), 1657 (C=N, str.), 1598 (C=N, pyridine str.), 1562 (C=C, ar.), 1402 (C-C, ar.), 749 and 711 (C-H ar. bend.) cm^{-1}. IR data provide the evidence for the formation of C=N in the ligand. One can easily find that in the

IR spectra of dafone, which contains a carbonyl group, there is a peak at 1716 cm^{-1} corresponding to the C=O vibration band that it disappears in the new ligand. In the IR spectrum of ligand (N-(4,5-diazafluoren-9-ylidene)aniline), there appears a new peak (ca. 1657 cm^{-1}) instead of the peak 1716 cm^{-1}. We assign this new peak to C=N vibration. This clearly shows that new ligand (dian) has been formed, and the condensation has occurred.

The IR spectrum of the complex (as can be seen in Fig. 2) represents bands similar to those of ligand with a slight shift to the lower wave number owing to its coordination with Ag(I) metal center in the complex. For example, the characteristic band at 1652 cm^{-1} and 1591 cm^{-1} can be assigned to C=N stretching vibration of ligand that it appears in free ligand at about 1657 cm^{-1} and 1598 cm^{-1}, respectively. This can be repeat for other bands showing that coordination to the metal through the nitrogen atom is expected to reduce electron density in the ligand as a result of the withdrawing of electron density from the N atom and diminish the C=N absorption frequency. The infrared absorption band of the anion in this complex shows that the nitrate isn't coordinated to Ag(I) center. This fact was inferred from the strong new band revealed at 1338 cm^{-1} [30].

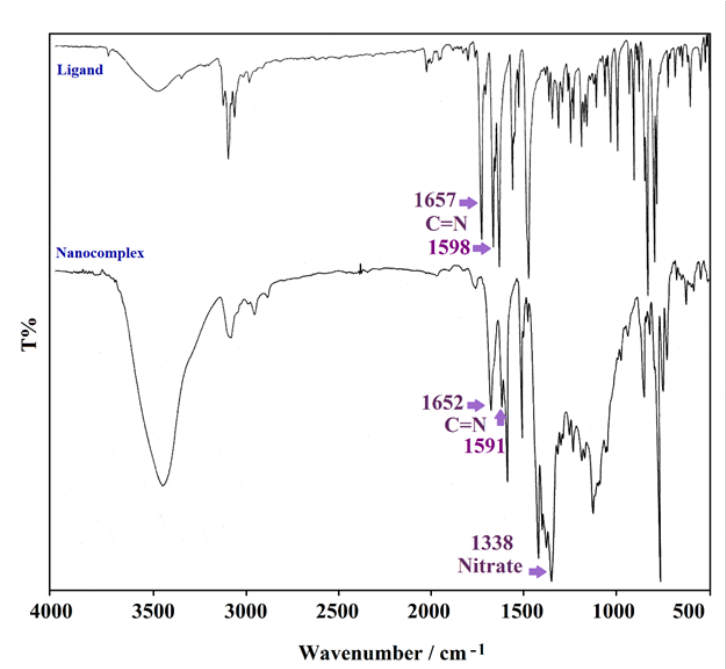

Fig. 2. FT-IR spectra of the free ligand and Ag(I) nanocomplex

3.2.2. NMR Spectral Studies

^{1}H NMR spectrum of ligand in $CDCl_3$ (Fig. 3) shows aromatic protons at 8.82 (d, H4), 8.66 (d, H3), 8.26 (d, H6), 7.46 (t, H7 and H11), 7.41 (dd, H5), 7.28 (t, H9), 7.01 (dd, H8 and H10), 6.98 (t, H2) and 6.87 (d, H1) (The protons have been numbered in scheme 1), which is consistent with literature [24]. In order to assign the chemical shifts in ligand, it must be noted that the protons in the two pyridine rings of the bipyridine ligands are not equivalent

because of sp^2 hybridization of the N atom in the aniline moiety. The differences in the quantities of the chemical shifts can be related to the interaction of the protons with the lone pair on the nitrogen of the aniline. The protons in the ring closer to the lone pair are shifted upfield, but the protons in the ring further from the nitrogen lone pair are shifted downfield [24], it can interpret large difference in chemical shifts of the proton number 1 and 6. The effect on the chemical shifts decreases in relation to their distance from the source of the effect. The distance of the protons from the benzene ring and its chemical shift are also related. The shifts are similar to proton chemical shifts of [10]-paracyclophane ascribed to ring current effects [24].

The proton NMR spectra of transition-metal complexes with heterocyclic ligands are complex and their interpretations accompany with difficulty. Complexation between ligand and metal center causes changes in the chemical shift of ^{1}H NMR of ligands. Decreasing in the electron density of the ligand rings by the σ effect gives downfield shifts at all ring positions. The values of the shifts are inversely proportionate to the distance from the metal. On the other hand, π-back-bonding from the d orbitals of the metal into the π system of ligand increases the π density of the carbons in the ring, which yields an upfield change in the chemical shift of the ring protons. The σ effect of the remote sites is smaller than others, so for metals that have significant π-back-bonding to the ligand, shielding is expected [31].

The ^{1}H NMR spectrum of the nanocomplex in the same solvent is consistent with the proposed formula. It represents similar resonances to ligand with a shift owing to coordination to the metal center. In this case, the chemical shifts for protons in all positions shift downfield compared with the free ligand, as a result of σ donation. ^{1}H NMR spectrum of nanocomplex in $CDCl_3$ (Fig. 4) shows aromatic protons at 9.01 (d, H6), 8.84 (d, H3, H4), 8.58 (d, H1), 8.05 (d, H7 and H11), 7.42 (m, H8, H9 and H10), 7.26 (t, H5), 7.06 (dd, H2).

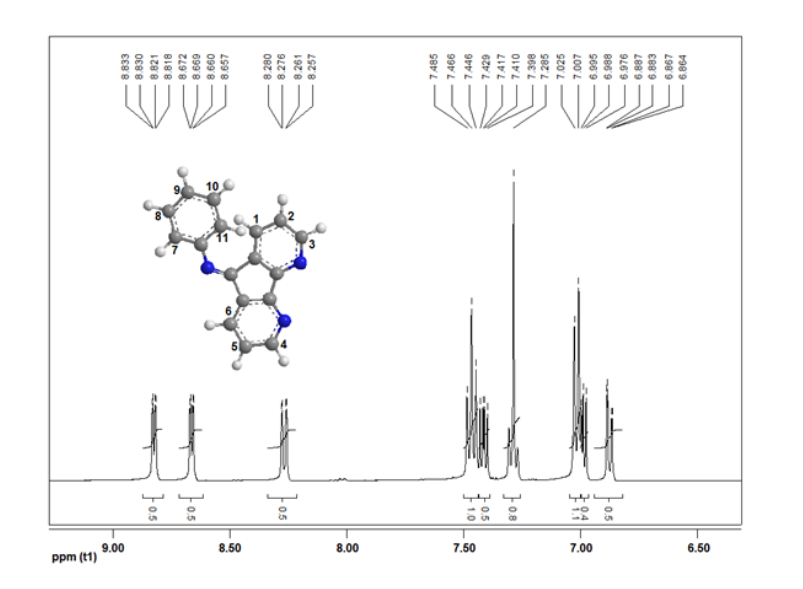

Fig. 3. ^{1}HNMR spectrum of the dian at room temperature in $CDCl_3$

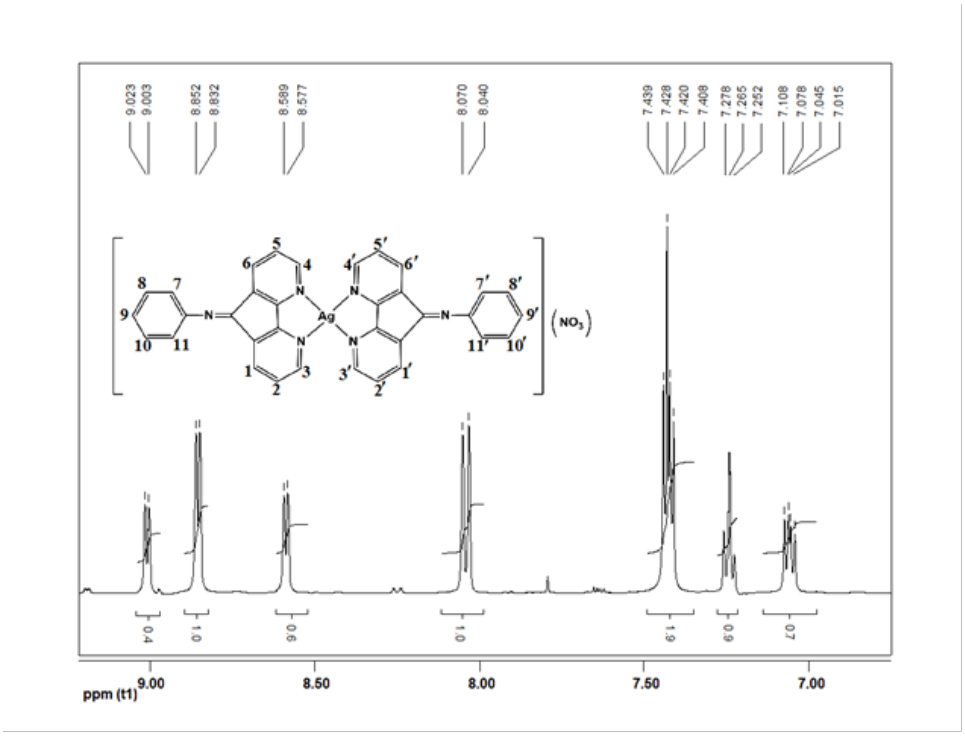

Fig. 4. ^{1}HNMR spectrum of the $[Ag(dian)_2]NO_3$ at room temperature in $CDCl_3$

3.3. Electrocatalytic oxidation of norepinephrine at a Ag(I)/SPE

The electrochemical behavior of norepinephrine is dependent on the pH value of the aqueous solution. Therefore, pH optimization of the solution seems to be necessary in order to obtain the electrocatalytic oxidation of epinephrine. Thus the electrochemical behavior of norepinephrine was studied in 0.1 M PBS in different pH values (2.0<pH<9.0) at the surface of Ag(I)/SPE by CV. It was found that the electrocatalytic oxidation of norepinephrine at the surface of Ag(I)/SPE was more favored under neutral conditions than in acidic or basic medium. Thus, the pH 7.0 was chosen as the optimum pH for electrocatalysis of norepinephrine oxidation at the surface of Ag(I)/SPE.

Fig. 5 depict the cyclic voltammetric responses for the electrochemical oxidation of 200.0 μM norepinephrine at Ag(I)/SPE (curve a) and bare SPE (curve b). The anodic peak potential for the oxidation of norepinephrine at Ag(I)/SPE (curve a) is about 200 mV compared with 250 mV for that on the bare SPE (curve b). Similarly, when the oxidation of norepinephrine at the Ag(I)/SPE (curve a) and bare SPE (curve b) are compared, an extensive enhancement of the anodic peak current at Ag(I)/SPE relative to the value obtained at the bare SPE (curve b) is observed. In other words, the results clearly indicate that the Ag(I) nanocomplex improve the norepinephrine oxidation signal.

The effect of potential scan rates on the oxidation current of norepinephrine has been studied (Fig. 6). The results showed that increasing in the potential scan rate induced an increase in the peak current. In addition, the oxidation process is diffusion controlled as

deduced from the linear dependence of the anodic peak current (I_p) on the square root of the potential scan rate ($\nu^{1/2}$) over a wide range from 10 to 500 mV s^{-1} (Fig. 7). The total electro reaction of norepinephrine at Ag(I)/SPE is shown in Scheme 2.

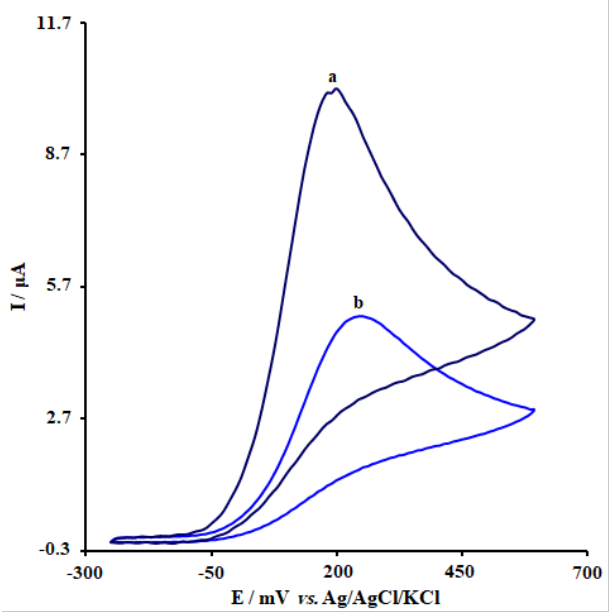

Fig. 5. Cyclic voltammograms of (a) Ag(I)/SPE and (b) bare SPE in 0.1 M PBS (pH 7.0) in the presence of 200.0 µM norepinephrine at the scan rate 50 mVs^{-1}

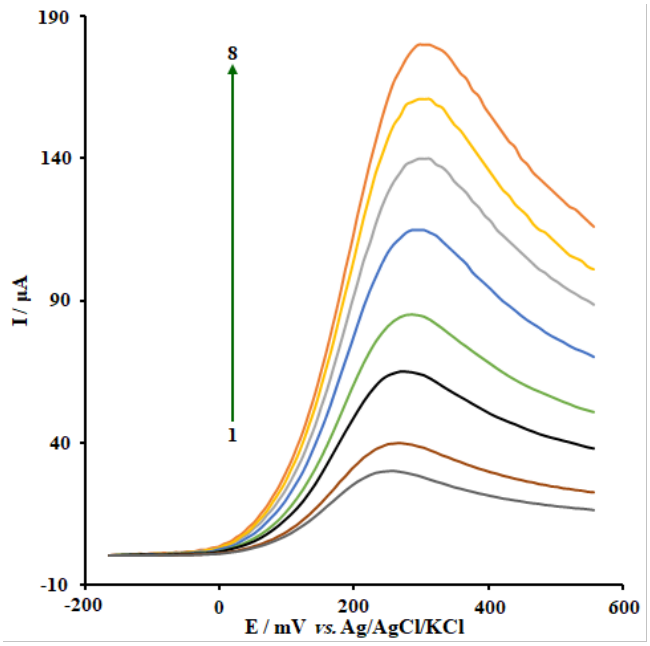

Fig. 6. Cyclic voltammograms of Ag(I)/SPE in 0.1 M PBS (pH 7.0) containing 200.0 µM norepinephrine at various scan rates; numbers 1-8 correspond to 10, 20, 60, 100, 200, 300, 400 and 500 mV s^{-1}, respectively

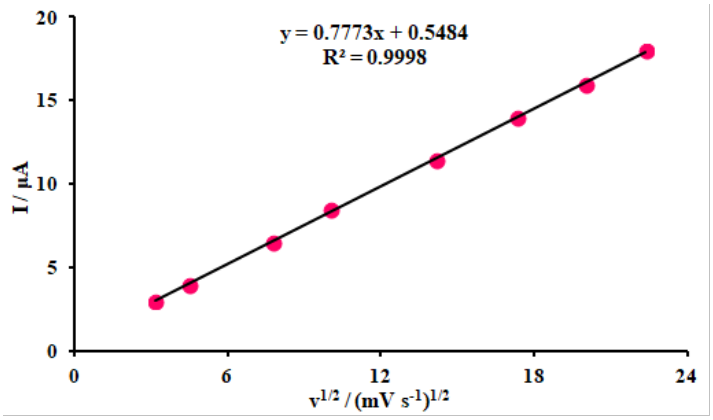

Fig. 7. Variation of cathodic peak current *vs.* $\nu^{1/2}$

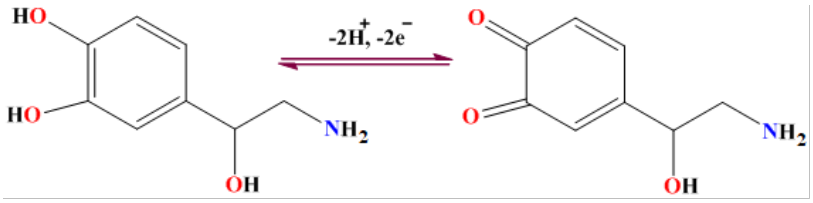

Scheme 2. Electro-oxidation mechanism of norepinephrine at modified electrode

3.4. Chronoamperometric measurements

Chronoamperometric measurements of amitriptyline at Ag(I)/SPE were carried out by setting the working electrode potential at 0.3 V for the various concentration of amitriptyline in PBS (pH 7.0) (Fig. 8).

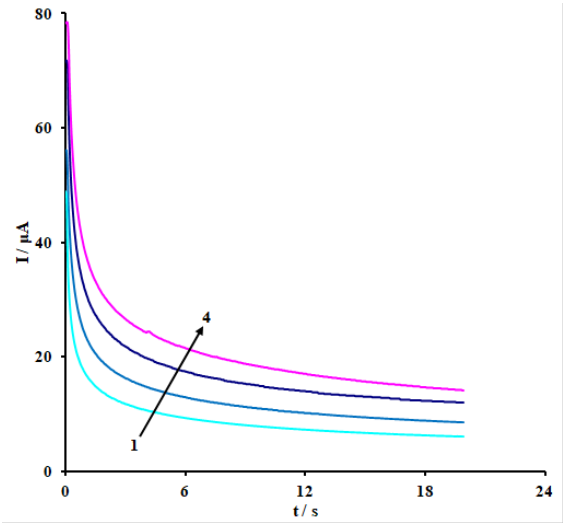

Fig. 8. Chronoamperograms obtained at Ag(I)/SPE in 0.1 M PBS (pH 7.0) for different concentration of norepinephrine. The numbers 1–4 correspond to 0.1, 0.7, 1.5 and 2.0 mM of norepinephrine

For an electroactive material (norepinephrine in this case) with a diffusion coefficient of D, the current observed for the electrochemical reaction at the mass transport limited condition is described by the Cottrell equation [32].

$$I = nFAD^{1/2}C_b\pi^{-1/2}t^{-1/2}$$

Where D and C_b are the diffusion coefficient ($cm^2\ s^{-1}$) and the bulk concentration (mol cm^{-3}), respectively. Experimental plots of I *vs.* $t^{-1/2}$ were employed, with the best fits for different concentrations of norepinephrine (Fig. 9A). The slopes of the resulting straight lines were then plotted *vs.* amitriptyline concentration (Fig. 9B). From the resulting slope and Cottrell equation the mean value of the D was found to be 4.9×10^{-6} cm^2/s.

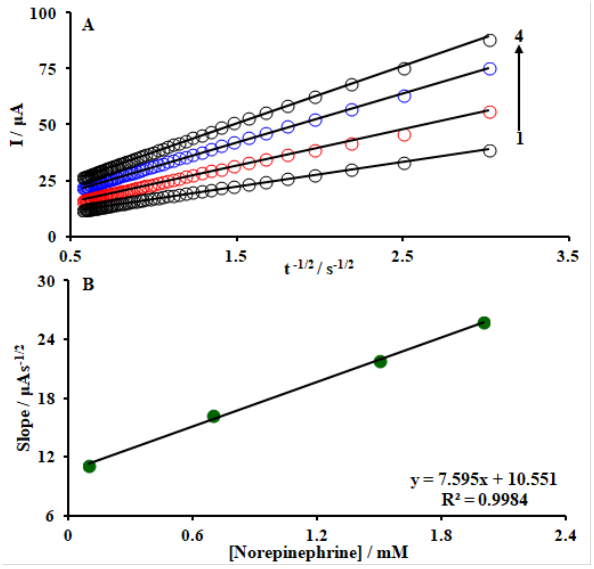

Fig. 9. (A) Plots of I *vs.* $t^{-1/2}$ obtained from chronoamperograms 1–4; (B) Plot of the slope of the straight lines against norepinephrine concentration.

3.5. Calibration plot and limit of detection

The peak current of norepinephrine oxidation at the surface of the modified electrode can be used for determination of norepinephrine in solution. Therefore, differential pulse voltammetry (DPV) experiments were done for different concentrations of norepinephrine (Initial potential=-0.1 V, End potential=0.55 V, Step potential=0.1 V, Modulation amplitude=0.02505 V). The oxidation peak currents of norepinephrine at the surface of a modified electrode were proportional to the concentration of the norepinephrine within the ranges 1.0 to 300.0 µM (Fig. 10). The detection limit (3σ) of norepinephrine was found to be 6.0×10^{-7} M.

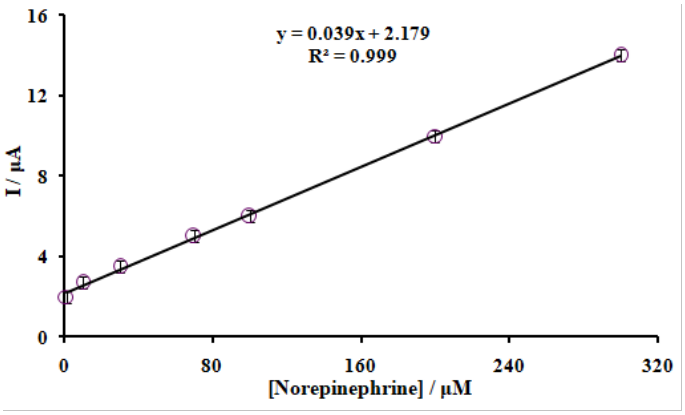

Fig. 10. Plot of the electrocatalytic peak current as a function of norepinephrine concentration in the range of 1.0-300.0 µM

4. CONCLUSION

A new silver(I) nanocomplex, $[Ag(dian)_2]NO_3$ and dian ligand have been prepared and fully characterized. The Ag(I) nanocomplex coated on the surface of graphite screen printed electrode, and the as-prepared modified Ag(I)/SPE electrode was used to detect norepinephrine in aqueous solutions, thus demonstrating the electroanalytical application of the Ag(I) nanocomplex. The Ag(I)/SPE showed a faster electron transfer rate and better electrocatalytic oxidation abilities towards norepinephrine than the bare graphite screen printed electrode. The detection limit of norepinephrine could be as low as 0.6 µM, with a linear range from 1.0 to 300.0 µM.

REFERENCES

[1] S. Sheikh, S. E. Haque, and S. S. Mir, J. Neurodegen. Diseases 8 (2013) 563481.
[2] N. G. Mphuthi, A. S. Adekunle, and E. E. Ebenso, Sci. Rep. 6 (2016) 26938.
[3] P. Rosy, S. K. Yadav, B. Agrawal, M. Oyama, and R. N. Goyal, Electrochim. Acta 125 (2014) 622.
[4] Y. Yui, Y. Itokawa, and C. Kawai, Anal. Biochem. 108 (1980) 11.
[5] R. N. Goyal, and S. Bishnoi, Talanta 84 (2011) 78.
[6] R. S. K. Yadav, B. Agrawal, M. Oyama, and R. N. Goyal, Electrochim. Acta 125 (2014) 622.
[7] X. Ma, M. Chen, X. Li, A. Purushothaman, and F. Li, Int. J. Electrochem. Sci. 7 (2012) 991.
[8] M. P. O'Halloran, M. Pravda, and G. G. Guilbault, Talanta 55 (2001) 605.
[9] Sh. Jahani, and H. Beitollahi, Anal. Bioanal. Electrochem. 8 (2016) 158.
[10] Y. Mu, D. Jia, Y. He, Y. Miao, and H. L. Wu, Biosens. Bioelectron. 26 (2011) 2948.
[11] H. Beitollahi, S. Tajik, and Sh. Jahani, Electroanalysis 28 (2016) 1093.

[12] M. P. Deepak, M. P. Rajeeva, and G. P. Mamatha, Anal. Bioanal. Electrochem. 8 (2016) 931.
[13] Sh. Jahani, and H. Beitollahi, Electroanalysis 28 (2016) 2022.
[14] O. Dominguez Renedo, M. A. Alonso-Lomillo, and M. J. Arcos Martinez, Talanta 73 (2007) 202.
[15] F. Soofiabadi, A. Amiri, and Sh. Jahani, Anal. Bioanal. Electrochem. 9 (2017) 340.
[16] J. Wang, J. Lu, S. B. Hocevar, and B. Ogorevc, Electroanalysis 13 (2001) 13.
[17] M.R. Ganjali, F. Garkani Nejad, H. Beitollahi, Sh. Jahani, M. Rezapour, and B. Larijani, Int. J. Electrochem. Sci. 12 (2017) 3231.
[18] H. Mahmoudi Moghaddam, H. Beitollahi, S. Tajik, Sh. Jahani, H. Khabazzadeh, and R. Alizadeh, Russ. J. Electrochem. 53 (2017) 452.
[19] F. Kurniawan, V. Tsakova, and V. M. Mirsky, Electroanalysis 18 (2006) 1937.
[20] M. Khatami, and S. Pourseyedi, IET Nanobiotechnology 9 (2015) 184.
[21] J. Hou, C. Xu, D. Zhao, and J. Zhou, Sens. Actuators B 225 (2016) 241.
[22] M. Khatami, R. Mehnipor, M. H. S. Poor, and G. S. Jouzani, J. Clust. Sci. 27 (2016) 1.
[23] Z. Azizi, S. Pourseyedi, M. Khatami, and H. Mohammadi, J. Clust. Sci. 27 (2016) 1613.
[24] Y. Wang, and D. P. Rillema, Tetrahedron 53 (1997) 12377.
[25] H. Cang, D. Jin, S. Q. Wang, S. Liua, and J. T. Wang, Acta Crystallogr. 64 (2008) 1221.
[26] A. J. Pallenberg, T. M. Marschner, and D. M. Barnhart, Polyhedron 16 (1997) 2711.
[27] A. A. Massoud, Y. M. Gohar, V. Langer, P. Lincoln, F. R. Svensson J. Jänis, S. Gardebjer, M. Haukka, F. Jonsson, E. Aneheim, P. Löwenhielm, M. A. M. Abu-Youssef, and L. R. Öhrström, New J. Chem. 35 (2011) 640.
[28] M. McCann, B. Coyle, S. McKay, P. McCormack, K. Kavanagh, M. Devereux, V. McKee, P. Kinsella, R. O'Connor, and M. Clynes, BioMetals 17 (2004) 635.
[29] W. J. Geary, Coordin. Chem. Rev. 7 (1971) 81.
[30] N. Shahabadi, S. Kashanian, and Z. Ahmadipour, DNA Cell Biol. 30 (2011) 187.
[31] C. R. Johnson, W.W. Henderson, and R. E. Shepherd, Inorg. Chem. 23 (1984) 2754.
[32] A. J. Bard, and L. R. Faulkner, Electrochemical Methods Fundamentals and Applications, second ed, Wiley, New York (2001).